Am J Cancer Res 2024;14(11):5504-5520
www.ajcr.us /ISSN:2156-6976/ajcr0158835

Original Article

The small protein LINC01547-ORF inhibits colorectal cancer progression by regulating the CLDN18-FAK-AKT axis

Shuai Zhang[1], Siguang Xu[1], Dandan Li[2], Songxin Wu[1], Miaomiao Han[1], Yifei Han[1], Zixi Wang[1], Dan Qiao[1], Hang Yuan[1], Baoshun Du[3], Hongwei Chen[2], Zheying Zhang[1]

[1]Department of Pathology, School of Basic Medical Sciences, Xinxiang Medical University, Xinxiang 453003, Henan, China; [2]Department of Emergency Center Emergency Critical Care, The Fourth Clinical College of Xinxiang Medical College, Xinxiang 453003, Henan, China; [3]Second Department of Neurosurgery, Xinxiang Central Hospital, Xinxiang 453003, Henan, China

Received June 28, 2024; Accepted November 14, 2024; Epub November 15, 2024; Published November 30, 2024

Abstract: Long non-coding RNA (lncRNA)-encoded small proteins play a major role in colorectal cancer. To identify more functional encoded small proteins, ribosome profiling data from colorectal cancer (CRC) cells were screened for ribosome-associated lncRNAs. The search identified LINC01547 that was shown to encode a small protein of 76 amino acids, termed LINC01547-ORF. Real-time quantitative fluorescence showed that LINC01547 expression was downregulated in colorectal cancer tissues. However, cell functional assays revealed that LINC01547 inhibited the proliferation and migration of colorectal cancer cell lines. Meanwhile, western blot and immunofluorescence assays confirmed that LINC01547 encoded LINC01547-ORF. Cellular functional assays indicated that compared with LINC01547 itself, LINC01547-ORF inhibited the proliferation and migration of colorectal cancer cell lines. Gene set enrichment analysis identified enrichment in the focal adhesion pathway and association with CLDN18 protein, whereas protein molecular docking models revealed interacting domains and amino acid residue sites. Of note, co-immunoprecipitation and immunofluorescence experiments showed that LINC01547-ORF could bind to the CLDN18 protein and that this interaction reduced CLDN18 ubiquitination, thereby promoting protein expression. Finally, western blot and immunofluorescence assays confirmed that LINC01547-ORF could target CLDN18 to inhibit the FAK/PI3K/AKT signaling pathway, suppressing colorectal cancer cell development. These findings suggest that the LINC01547-ORF-encoded small protein inhibits proliferation and migration in colorectal cancer, thereby offering a promising direction for treating this disease.

Keywords: Colorectal cancer, LINC01547-ORF, CLDN18, FAK, PI3K/AKT

Introduction

Colorectal cancer (CRC), one of the most common malignancies, ranks third in incidence among global cancers, with its mortality rate exhibiting an increasing trend [1]. Approximately 60% of patients newly diagnosed with CRC develop metastases, the primary cause of death in these individuals. The underlying mechanisms of CRC tumor development remain unclear [2]. In particular, the function of long noncoding RNA (lncRNA)-derived microproteins in CRC is poorly understood, and the characterization of these microproteins may provide insights into the molecular regulatory networks involved in CRC progression [3, 4].

A class of eukaryotic non-coding RNA molecules > 200 nucleotides in length, lncRNAs perform several biological functions [5]. Indeed, they are involved in regulating genomic imprinting, stem cell pluripotency, and various other biological and physiological processes [6]. Data from the Encyclopedia of DNA Elements project indicate that there are many lncRNA transcripts in addition to protein-coding genes [7, 8]. Recent studies have revealed that such lncRNAs may contain one or several short open reading frames (sORFs) capable of encoding microproteins and

https://doi.org/10.62347/PNKH7683

peptides < 100 amino acids in size, which are difficult to detect [9-13]. In the past 5 years, with the advancement of high-throughput sequencing technologies, research on the mechanism of lncRNA-encoded microproteins has produced many groundbreaking findings [14, 15]. These studies have revealed that lncRNA-encoded microproteins can regulate homeostasis, cancer progression, disease development, embryogenesis, and other vital physiological processes via their participation in mitochondrial metabolism regulation, transcriptional control, translational regulation, mRNA splicing, signal transduction, and cell senescence [10, 12, 16, 17].

The extracellular matrix (ECM) receptor interaction pathway involves several interactions and signaling processes between the cells and ECM, a complex noncellular component comprising proteins and polysaccharides that provides structural support to cells and regulates cellular behavior. This pathway involves various molecules, including integrins, CD44, and MMPs, among others. Integrins are a large family of transmembrane receptors composed of α and β subunits that interact with various proteins in ECM, such as fibronectin, laminin, and collagen [18, 19]. Integrins activation can trigger multiple signaling pathways, such as FAK/PI3K/AKT, thereby influencing cellular behavior. The focal adhesion pathway involves many molecular interactions and signaling processes within the cell that regulate the formation and disassembly of focal adhesions. Its key components are integrins and focal adhesion kinase (FAK). On integrin activation, FAK accumulates at focal adhesion sites and initiates downstream signaling pathways via phosphorylation [20].

The protein CLDN18, highly expressed in the focal adhesion pathway, is a tight junction protein that helps maintain epithelial barrier functions and regulate cell polarity. Under normal physiological conditions, it is exclusively expressed on the differentiated epithelial cells of the gastric mucosa and is not found on other healthy tissues. However, its expression is upregulated in gastric cancer and pancreatic cancer as well as in primary malignancies such as breast cancer, CRC, and liver cancer [21]. However, the role of claudins in carcinogenesis is unclear. The CLDN18 gene can be aberrantly activated and selectively and stably expressed in specific tumor tissues, thereby participating in tumor cell proliferation, differentiation, and migration. Thus, CLDN18 may be a potential target for treating the malignant tumors of the digestive system [22-24].

FAK is a nonreceptor cytoplasmic protein tyrosine kinase and member of the protein tyrosine kinase superfamily. It plays a significant role in cell signal transduction, acting as a central hub for signals entering and leaving the cell and mediating multiple signaling pathways [25, 26]. FAK received signals from integrins, growth factors, and mechanical stimuli to activate certain intracellular signaling pathways. Upon activation, FAK forms a complex with Src, and its Tyr397 directly binds with the SH2 domain of PI3K, which then activates AKT to regulate cell growth [26, 27]. In addition, FAK can induce PI3K/AKT signaling cascade, leading to upregulation of EMT markers [28]. Indeed, the FAK/PI3K/AKT pathway is closely associated with the regulation of cell growth [25, 26, 29-31]. Meanwhile, the epithelial-mesenchymal transition is a biological process in which epithelial cells lose their characteristics and gain several mesenchymal cell features, including enhanced migratory capacity, invasiveness, and resistance to apoptosis [20].

In view of the important regulatory role of peptide or small protein-encoding lncRNAs in tumors, future studies should not only consider lncRNA as an important regulatory RNA but also fully explore small ORFs on these lncRNAs to assess whether they encode functional peptides and small proteins. These biomolecules can be used as novel anticancer therapeutic targets as well as diagnostic and prognostic cancer markers to improve the overall effectiveness of cancer diagnosis and treatment.

In the present study, a 76-amino-acid microprotein encoded by LINC01547, named LINC01547-ORF, was identified and its impact on the proliferation and migration of CRC cell lines was explored. In addition, whether LINC01547-ORF inhibits CRC growth by regulating the CLDN18-FAK-AKT axis was evaluated.

Materials and methods

Cell culture

The human CRC cell lines LOVO, DLD-1, HCT-8, HCT-116, SW620, and SW480 and the normal intestinal mucosal epithelial cell line FHC were

Table 1. Data statistics of CRC patients

Clinicopathological variables	N	percentage
Age (years)		
≤ mean (57)	10	(62.5%)
> mean (57)	6	(37.5%)
Sex		
Male, n (%)	8	(50%)
Female, n (%)	8	(50%)
AJCC TNM classification		
I, n (%)	2	(12.5%)
II, n (%)	6	(37.5%)
III, n (%)	5	(31.25%)
IV, n (%)	3	(18.75%)
Lynph Metastasis		
Yes, n (%)	7	(43.75%)
No, n (%)	9	(56.25%)
Distant Metastasis		
Yes, n (%)	4	(25%)
No, n (%)	12	(75%)

purchased from the American Type Culture Collection. The cells were cultured in DMEM, supplemented with 10% fetal bovine serum, in an incubator at 37°C and 5% CO_2. All cell lines were authenticated prior to their culture and tested for mycoplasma contamination every 3 months. HCT-116 (ATCC-CCL 247), HCT-8 (ATCC-CCL 244), SW480 (ATCC-CCL 228), SW620 (ATCC-CCL 227), RKO (ATCC-CRL 2577), LOVO (ATCC-CCL 229), DLD-1 (ATCC-CCL 221), CACO2 (ATCC-HTB 37), and FHC (ATCC-CRL 1831).

Tissue samples

The present study analyzed 16 pairs of tissues from patients with CRC, including 8 female and 8 male patients (**Table 1**). The patients had no other symptoms and had not received treatment. The CRC and paired adjacent healthy (5 cm from the tumor edge) tissues were collected by professional technicians from patients undergoing CRC surgery at the First Affiliated Hospital of Xinxiang Medical University from January 2021 to April 2022. All study procedures were approved by the Ethics Committee of Xinxiang Medical University. The tissues were snap-frozen in liquid nitrogen within 10 min of excision and then stored at -80°C. The number of the ethics approval letter: No. XYLL-2020126.

Western blot assay

Proteins were first extracted using lysis buffer (Beyotime Biotechnology) containing 100× protease inhibitors (Beyotime Biotechnology) and then quantified using a bicinchoninic acid protein assay kit (KeyGen Biotech) following the manufacturer's instructions. 20 μg total proteins were separated via 15% SDS-PAGE and transferred to PVDF membranes (Roche), which were blocked with 5% nonfat milk at room temperature for two hours to prevent nonspecific binding. The membranes were initially incubated with primary antibodies at 4°C overnight, then washed three times, and subsequently incubated with the corresponding secondary antibodies at room temperature for 1 h. Finally, protein bands were detected with the Pierce ECL Western Blotting Substrate (Thermo Scientific) and analyzed via densitometry using the ImageJ software. Additional details on the antibodies are provided in Table S1. (FLAG (DYKDDDDK): Proteintech, 80010-1-RR, WB: 1:50000, 17 KD, rabbit); (CLDN18: Proteintech, 66167-1-Ig, WB: 1:700, 28 KD, mouse); (p-FAK: Affinity, AF3398, WB: 1:1000, 119 KD, rabbit); (FAK: Proteintech, 12636-1-AP, WB: 1:1000, 119 KD, rabbit); (P-PI3K: Affinity, AF3241, WB: 1:1000, 80 KD, rabbit); (PI3K: Proteintech, 60225-1-Ig, WB: 1:1500, 85 KD, mouse); (P-AKT: Proteintech, 28731-1-AP, WB: 1:2000, 58 KD, rabbit); (AKT: Proteintech, 10176-2-AP, WB: 1:5000, 56 KD, rabbit); (GAPDH: Proteintech, 60004-1-Ig, WB: 1:50000, 36 KD, mouse).

RNA extraction and RT-qPCR

Total RNA was extracted from each sample using the TRIzol reagent and was then isolated using chloroform, precipitated with isopropanol, washed with 75% ethanol and dissolved in DEPC water. cDNA was synthesized from total RNA using a reverse transcription kit (Servicebio, Wuhan, China), and qPCR was performed with the SYBR Green dye (Vazyme, Nanjing, China). The qPCR amplification conditions were as follows: an initial denaturation at 95°C for 10 min, followed by denaturation at 95°C for 15 s; annealing/extension at 60°C for 1 h; and a melting curve analysis at 95°C for 15 s and 60°C for 1 min for 40 cycles. The results were normalized to the expression of GAPDH using the $2^{-\Delta\Delta Ct}$ method as previously described

[32]. We calculate the difference of the target gene ΔCt (ΔΔCt) between the experimental sample and the control sample, and then use the formula 2^-ΔΔCt to calculate the multiple of change in the expression of the target gene in the experimental sample relative to the control sample. All primers are NCBI validated and purchased from sangon (Shanghai, China). We opened the official website of NCBI, entered the target sequence in the Prime-blast page, then set Primer parameters, and selected the database and species. We run prime-blast and get the results. The primer sequences were as follows: LINC01547 forward 5'-TTACAAACCCCAGTCCCAGC-3' and reverse 5'-ACTCAGAGCTTCTGTCCAGC-3'; CLDN18 forward 5'-GTGGTTTCACTGATTGGGATTG-3' and reverse 5'-GTTGTTGTACAAGTCTTGGGTG-3'; and GAPDH forward 5'-CAAGGCTGTGGGCAAGGTCATC-3' and reverse 5'-GTGTCGCTGTTGAAGTCAGAGGAG-3'.

Cell transfection

All cells were passaged when they reached 80%-90% confluence. In particular, HCT-116 and SW480 cells were digested with 0.25% trypsin, centrifuged, and resuspended in serum-free medium. The following day, at 70%-80% confluence, the medium was replaced with serum-free medium and cells were transfected with the appropriate plasmids (300-500 μg/ml) or siRNA (10 μm) using Lipofectamine 8000 (Beyotime Biotechnology, Shanghai, China) according to the manufacturer's instructions. After 6-8 hours of cultivation at 37°C and 5% CO_2, the cells were observed and the medium was replaced with serum-containing medium. The transfected cells cultured for 48-72 h were collected for follow-up experiments. The sequences of LINC01547 siRNA fragment 1 were forward 5'-CAAGAGACAACAGCGAUUATT-3' and reverse 5'-UAAUCGCUGUUGUCUCUUGTT-3' and those of siRNA fragment 2 were forward 5'-GCCACCUGCAGUUUCAUAATT-3' and reverse 5'-UUAUGAAACUGCAGGUGGCTT-3'. The sequences of CLDN18 siRNA fragment were forward 5'-GGACGAGGUACAAUCUUAUTT-3' and reverse 5'-AUAAGAUUGUACCUCGUCCTT-3'. The sequences of negative control siRNA fragment were forward 5'-UUCUCCGAACGUGUCACGUTT-3' and reverse 5'-ACGUGACACGUUCGGAGAATT-3'. LINC01547 siRNA, CLDN18 siRNA and negative control siRNA were all purchased from GenePharma (Shanghai, China). All plasmids were purchased from Tsingke (Beijing, China).

Cell counting kit-8 (CCK-8) assay

Cell proliferation capacity was assessed by using a CCK-8 kit (Beyotime Biotechnology) according to the manufacturer's instructions. SW480 and HCT-116 cells transfected with the plasmid LINC01547-ORF (pcDNA3.1-3xFlag) were inoculated into 96-well plates at a density of 2 × 10^3 cells/well, and 10 μL CCK-8 solution was added to each well on days 1-5. After incubation at 37°C for 2 h, absorbance was measured at 450 nm using enzyme-linked immunosorbent assay (Thermo, China) for 5 consecutive days. The experiments were performed in triplicate.

Transwell migration assay

SW480 and HCT-116 cells transfected with the plasmid LINC01547-ORF (pcDNA3.1-3xFlag) were cultured for 2 days, digested, centrifuged, and resuspended in serum-free medium for enumeration. Next, 4 × 10^4 cells were seeded into the upper chamber of a 24-well plate with 200 μL medium, and 700 μL FBS-supplemented medium was added to the lower chamber. After 24 h of incubation, the chambers were removed, and cells were fixed with 4% paraformaldehyde for 30 min at room temperature and stained with 1% crystal violet for 1 h at room temperature. The migrated cells were imaged and enumerated under an inverted microscope (8 μm pore size; Corning, NY, USA).

Colony formation assay

SW480 and HCT-116 cells transfected with LINC01547-ORF (pcDNA3.1-3xFlag) were inoculated into 6-well plates at a density of 500 cells/well and cultured for 10-14 days. The cells were fixed with 4% paraformaldehyde for 30 min at room temperature and stained with 1% crystal violet for 20 min at room temperature. Finally, cell colonies were photographed for analysis.

Wound healing assay

HCT-116 and SW480 cells were seeded at a density of 5 × 10^5 cells/well in a 6-well plate and cultured to 80% confluency by the following day. The cells were transfected with plasmid LINC01547-ORF (pcDNA3.1-3xFlag). A straight-line scratch was made in the center of the wells using a 200 μL pipette tip; three parallel scratches were made per well with three repli-

cates. After three washes with PBS, the cells were cultured in serum-free medium in an incubator at 37°C and 5% CO_2. Images were captured under an inverted microscope at 0 and 48 h, and wound area was calculated using imageJ to assess cell migration capability. First, the image is converted to a grayscale image, then the contrast is adjusted, the edges of the scratches are searched, a suitable threshold is set, and the measurement tool is used to calculate the area of the scratch region. We calculate 0 and 48 h wound areas. We calculated the migration rate by subtracting the 48 hour wound area from the 0 hour wound area and dividing it by the 0 hour wound area.

Immunofluorescence (IF) staining

SW480 and HCT-116 cells transfected with plasmids were allowed to adhere to culture plates and fixed with 4% paraformaldehyde for 30 min at room temperature. The cells were treated with 0.5% Triton X-100 for 20 min at room temperature and blocked with 5% bovine serum albumin at room temperature for 30 min. Next, a primary antibody was added to the cells and incubated at 4°C overnight. After three times of washing with PBS, they were incubated at room temperature with secondary antibody for 1 h and stained at room temperature with DAPI (Beyotime Biotechnology) for 10 min. Finally, the slides were treated with an anti-fading mounting medium and viewed under a confocal microscope (AR 1+, Nikon, Japan). (FLAG (DYKDDDDK): Proteintech, 80010-1-RR, IF: 1:100, rabbit); (CLDN18: Proteintech, 66167-1-Ig, IF: 1:100, mouse); (p-FAK: Affinity, AF3398, IF: 1:100, rabbit); (FITC: Proteintech, SA00003-2, IF: 1:100, rabbit); (FITC: Proteintech, SA00003-1, IF: 1:100, mouse); (Cy3: Proteintech, SA00009-2, IF: 1:100, rabbit).

Immunohistochemistry (IHC)

IHC was performed as per the kit instructions (Zhongshan Golden Bridge, Beijing, China). After incubation, the slides were dewaxed, antigen was retrieved, endogenous peroxidase activity was blocked at room temperature for 20 min, and holes were sealed. The primary antibody was then incubated overnight at 4°C according to the manufacturer's instructions, and then incubated at room temperature for 30 min with an enhanced secondary antibody polymer detection system. DAB was used for color development at room temperature for 3 min, followed by hematoxylin staining at room temperature for 1 min, differentiation, dehydration, and sealing. Images were captured under an inverted microscope. Two pathologists independently evaluated the slides and scored them. CLDN18 (1:50-400, Proteintech, 66167-1-Ig).

Co-immunoprecipitation (Co-IP)

Cell lysates from stable HCT-116 and SW480 cells were obtained after treating them with 300-500 μl lysis buffer (Beyotime Biotechnology) containing 100× protease inhibitors (Beyotime Biotechnology). Next, Co-IP was performed using antibodies against FLAG tag and immune complexes were captured via 25-50 μl Protein A/G Magnetic beads (HY-K0202, MCE). The magnetic beads were separated from the antibodies and washed four times with PBST (1× PBS+0.5% Tween-20). The magnetic beads and cell lysates were incubated in the turnover apparatus for 4°C overnight, and then washed four times. Elution buffer 60 μl was added to the magnetic beads at 95 degrees for 5 min. After separating the magnetic beads, the elution buffer is collected into the new EP tube. The complexes were assessed using western blot. FLAG (DYKDDDDK) (IP: 1:100, 21126-1-AP, Proteintech).

Gene set enrichment analysis (GSEA)

GSEA is a computational method that employs biological knowledge to interpret gene expression data. In the current study, data was first ranked according to the correlation of all genes with LINC01547-ORF expression. Then, a predefined set of genes were scored to obtain an enrichment score, which is a measure of the statistical evidence against the null hypothesis that its components are randomly distributed across the ranked list. Focal Adhesion (NES= 2.043), Ecm Receptor Interaction (NES=2.230), Cell Adhesion Molecules Cams (NES=2.350). GSEA was performed with The Cancer Genome Atlas (TCGA) CRC dataset offered by the Broad Institute of MIT using the GSEA software version 2.2.

Statistical analysis

Data and figures were respectively processed and analyzed by using the GraphPad Prism 8

and ImageJ software. For comparisons involving three or more groups, one-way analysis of variance (ANOVA) followed by Tukey's post hoc test was used to determine differences Student's t-test (two-tailed) or one-way ANOVA were used to calculate the difference between two groups or more than two groups. $P < 0.05$ was considered to indicate a statistically significant difference.

Results

LINC01547 inhibits CRC cell proliferation and migration

We used Translatome Database to obtain Ribo-seq data SRR7073127 (GSE142386) of colorectal cancer cell line HCT116, annotated lncRNAs, and intersected with screened differential lncRNAs. Differential lncRNAs that can bind to ribosomes are obtained (Tables S2 and S3). Ribo-seq data suggested that LINC01547 binds to the ribosome. Thus, 16 CRC tissues and their matched adjacent healthy tissues were analyzed for LINC01547 expression by using RT-qPCR, which showed that LINC01547 expression was downregulated in 13 CRC samples (**Figure 1A**). Meanwhile, RT-qPCR analysis performed for analyzing LINC01547 expression in eight CRC cell lines, including SW480, SW620, HCT-8, HCT-116, LOVO, RKO, DLD-1, and CACO2, and the normal intestinal mucosal epithelial cell line FHC revealed that LINC01547 expression was downregulated in CRC cells (*$P < 0.05$, **$P < 0.01$, ***$P < 0.001$, **Figure 1B**). To explore whether LINC01547 regulated the CRC cells phenotype, we selected HCT-116 and SW480 with relatively high expression of LINC01547 using siRNA. The targeting efficiency of si-LINC01547-1 and si-LINC01547-2 in the CRC cell lines HCT-116 and SW480 was confirmed via RT-qPCR, which revealed that the knockdown efficiency of the two siRNAs was > 70% (***$P < 0.001$, **Figure 1C**). Next, CCK-8, colony formation, transwell migration, and wound healing assays were used to assess the effect of LINC01547 on the proliferation and migration of HCT-116 and SW480 cells. The results indicated that after the siRNA-mediated knockdown of LINC01547, both cell proliferation and migration rates significantly increased, suggesting that LINC01547 inhibits CRC cell proliferation and migration (***$P < 0.001$, **Figure 1D-G**). These findings indicate that LINC01547 is downregulated in CRC tissues and cell lines and acts as an inhibitor in the proliferation and migration of CRC cells.

LINC01547 encodes a microprotein

To verify the coding potential of LINC01547 in CRC cell lines. The sequence of LINC01547 was retrieved, and the potential sORF was predicted using the EMBOSS: getorf website to obtain the amino acid sequence (Tables S2 and S3). A series of constructs (the plasmid pcDNA3.1-NC, pcDNA3.1-3xFlag, and pcDNA-3.1-3x Flag-mut) were generated and the plasmid LINC01547-ORF (pcDNA3.1-3xFlag) was transfected into CRC cell lines, followed by western blot using an antibody against the FLAG tag. The findings showed that LINC01547-ORF (pcDNA3.1-3xFlag) was highly expressed in CRC cell lines (**Figure 2A**).

To confirm the coding ability of LINC01547, plasmids pcDNA3.1-NC, pcDNA3.1-3xFlag, and pcDNA3.1-3xFlag-mut were transfected into the CRC cell lines LOVO, DLD-1, HCT-116, and SW480. Western blot indicated high microprotein expression in the pcDNA3.1-3xFlag group (**Figure 2B**). HCT-116 and SW480 cells, in which the microprotein was highly expressed, were selected for subsequent experiments. IF assays used to detect microprotein expression in CRC cell lines revealed a significant enhancement of staining in the pcDNA3.1-3xFlag group (**Figure 2C**). In summary, LINC01547 encoded the microprotein LINC01547-ORF.

LINC01547-ORF is not an lncRNA but inhibits CRC cells proliferation and migration

To investigate whether the effect of the microprotein LINC01547-ORF on CRC cells was dependent on LINC01547-based regulation, plasmids pcDNA3.1-NC, pcDNA3.1-3xFlag, and pcDNA3.1-3xFlag-mut were transfected into the CRC cell lines HCT-116 and SW480 with low LINC01547 expression. CCK-8, colony formation, transwell migration, and wound healing assays were performed to assess the effect of LINC01547-ORF on cell proliferation and migration (**$P < 0.01$, ***$P < 0.001$, **Figure 3A-D**). The results suggested that LINC01547-ORF is not the same as LINC01547 and that it inhibits CRC cell proliferation and migration.

LINC01547-ORF binds to CLDN18 protein

Gene set enrichment analysis (GSEA) revealed that the focal adhesion pathway, ECM, and cell

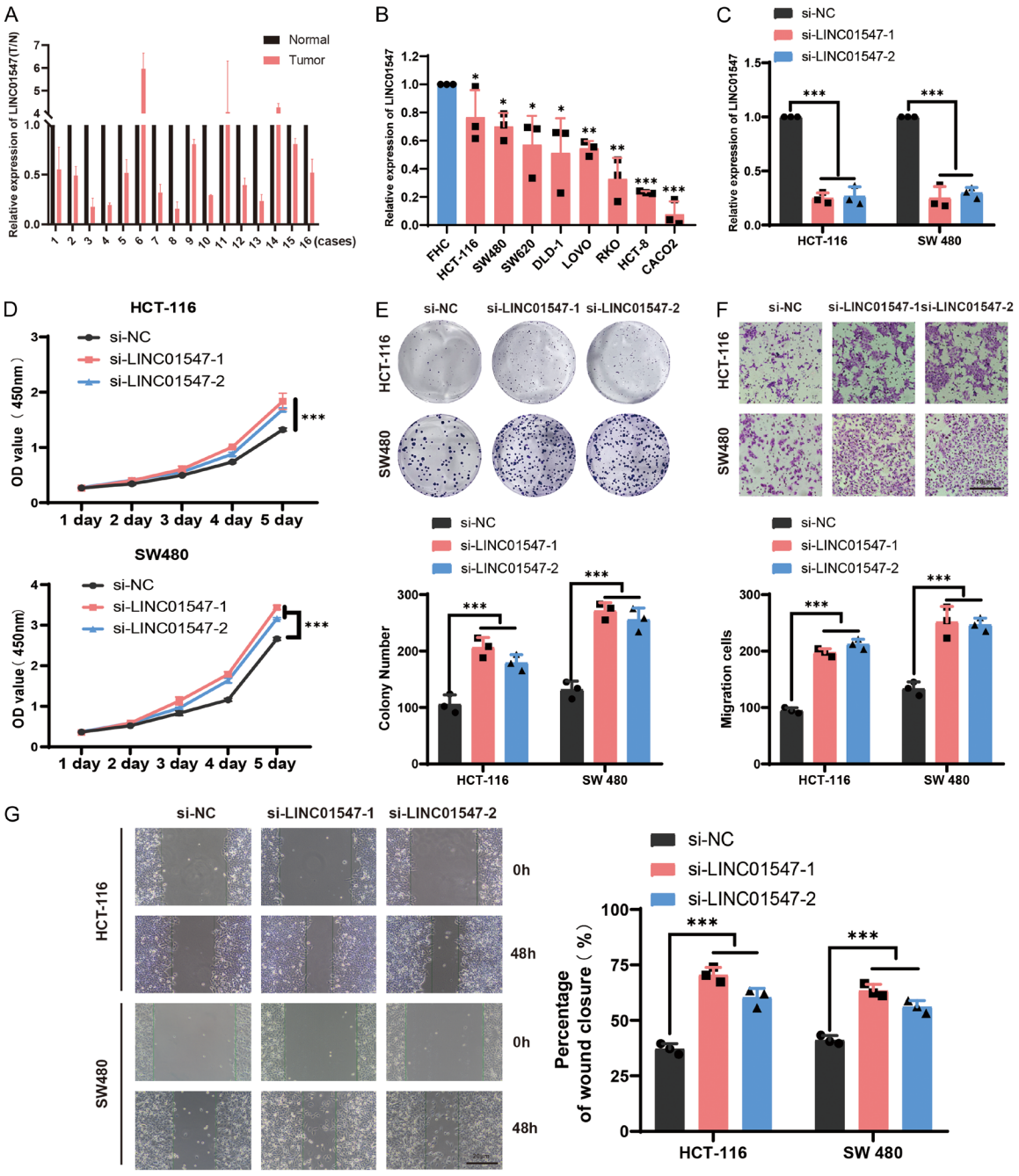

Figure 1. LINC01547 inhibits CRC cell proliferation and migration. A. RT-qPCR was used to validate the expression of LINC01547 in 16 colorectal cancer tissues and their matched normal adjacent tissues. B. RT-qPCR analysis of LINC01547 expression in CRC cells and the normal intestinal epithelial cell FHC. C. Two siRNAs targeting LINC01547 were used to completely abolish its expression. The efficiency of these siRNAs was verified by RT-qPCR. D, E. The effects of LINC01547 on the proliferation of CRC cell lines HCT-116 and SW480 were studied using CCK-8 and colony formation assays. F, G. Transwell migration assays and wound healing assays were performed to assess the impact of LINC01547 on the migratory abilities of CRC cell lines HCT-116 and SW480. *P < 0.05, **P < 0.01, ***P < 0.001.

adhesion molecule signaling pathway were related to LINC01547-ORF and the focal adhesion pathway CLDN18 and ECM protein COL6A6 were related to LINC01547-ORF (**Figure 4A**). To identify the target of LINC01547-ORF, the protein CLDN18 from the focal adhesion pathway

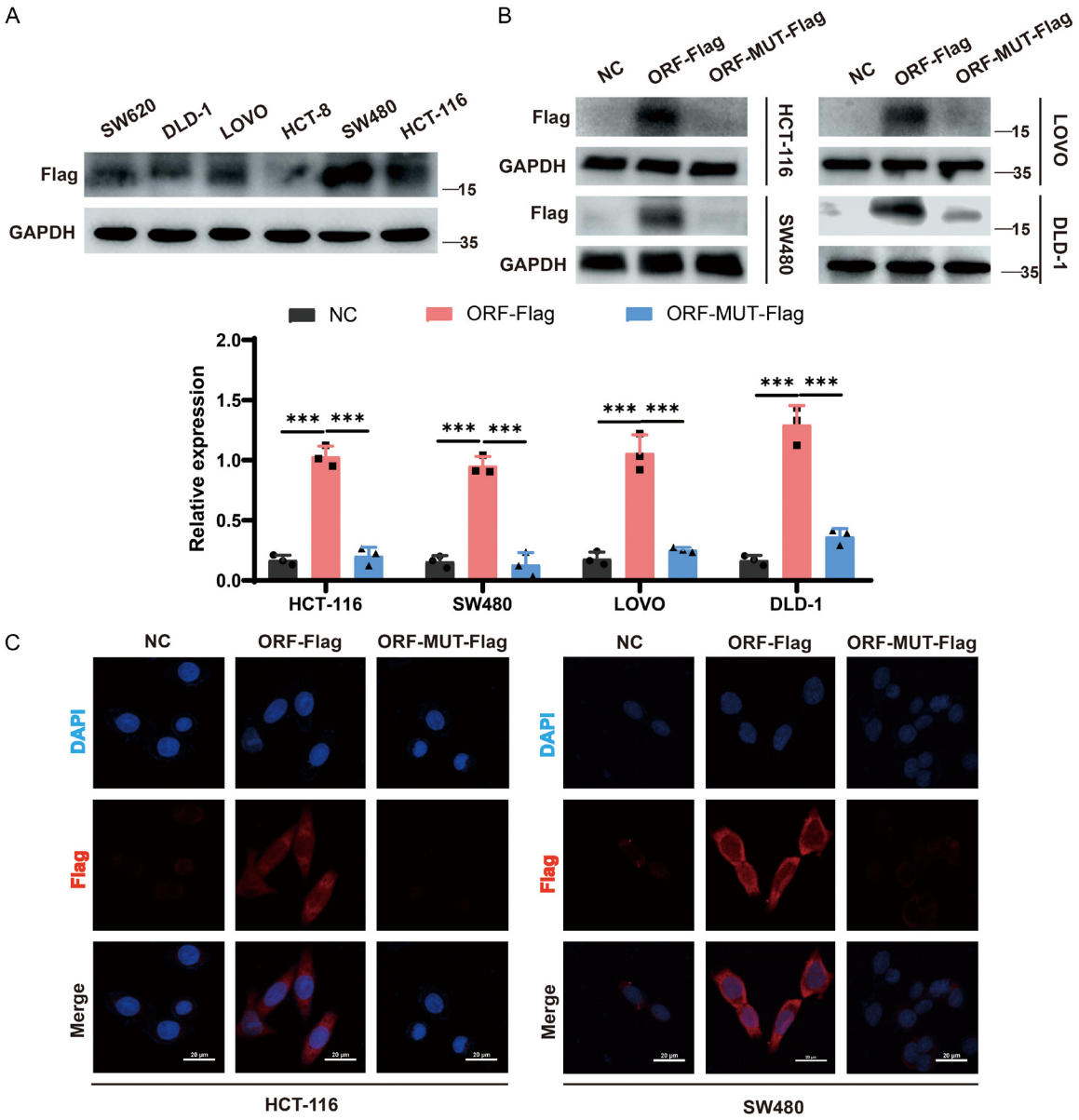

Figure 2. LINC01547 encodes a microprotein. A. Constructs of the plasmid pcDNA3.1-3xFlag were transfected into CRC cell lines, and protein expression was determined using a Flag antibody by Western blot after 48 hours. B. Constructs of pcDNA3.1-NC, pcDNA3.1-3xFlag, and pcDNA3.1-3xFlag-mut were transfected into CRC cell lines HCT-116, SW480, LOVO, and DLD-1, and protein expression was assessed by Western blot using a Flag antibody. C. High expression CRC cell lines HCT-116 and SW480 were transfected with pcDNA3.1-NC, pcDNA3.1-3xFlag, and pcDNA3.1-3xFlag-mut, and immunofluorescence using a Flag antibody was performed after 48 hours.

and COL6A6 from ECM proteins were investigated. Co-IP confirmed the interaction between LINC01547-ORF and CLDN18 in HCT-116 cells but not between LINC01547-ORF and COL6A6 (**Figure 4B**). Using AlphaFold2 on the Google Colab platform, the three-dimensional structure of the LINC01547-ORF microprotein was analyzed. In addition, the optimal model was retrieved to predict the interaction between LINC01547-ORF and CLDN18 to establish a protein docking model to obtain information on the interacting amino acid residues (LINC01547-ORF: red, CLDN18: green) (**Figure 4C**; Table S4). IF demonstrated the colocalization of LINC01547-ORF with CLDN18 in the cytoplasm (**Figure 4D**). Meanwhile, plasmids pcDNA3.1-NC, pcDNA3.1-3xFlag, and pcDNA3.1-3xFlag-mut were transfected into the CRC cell lines

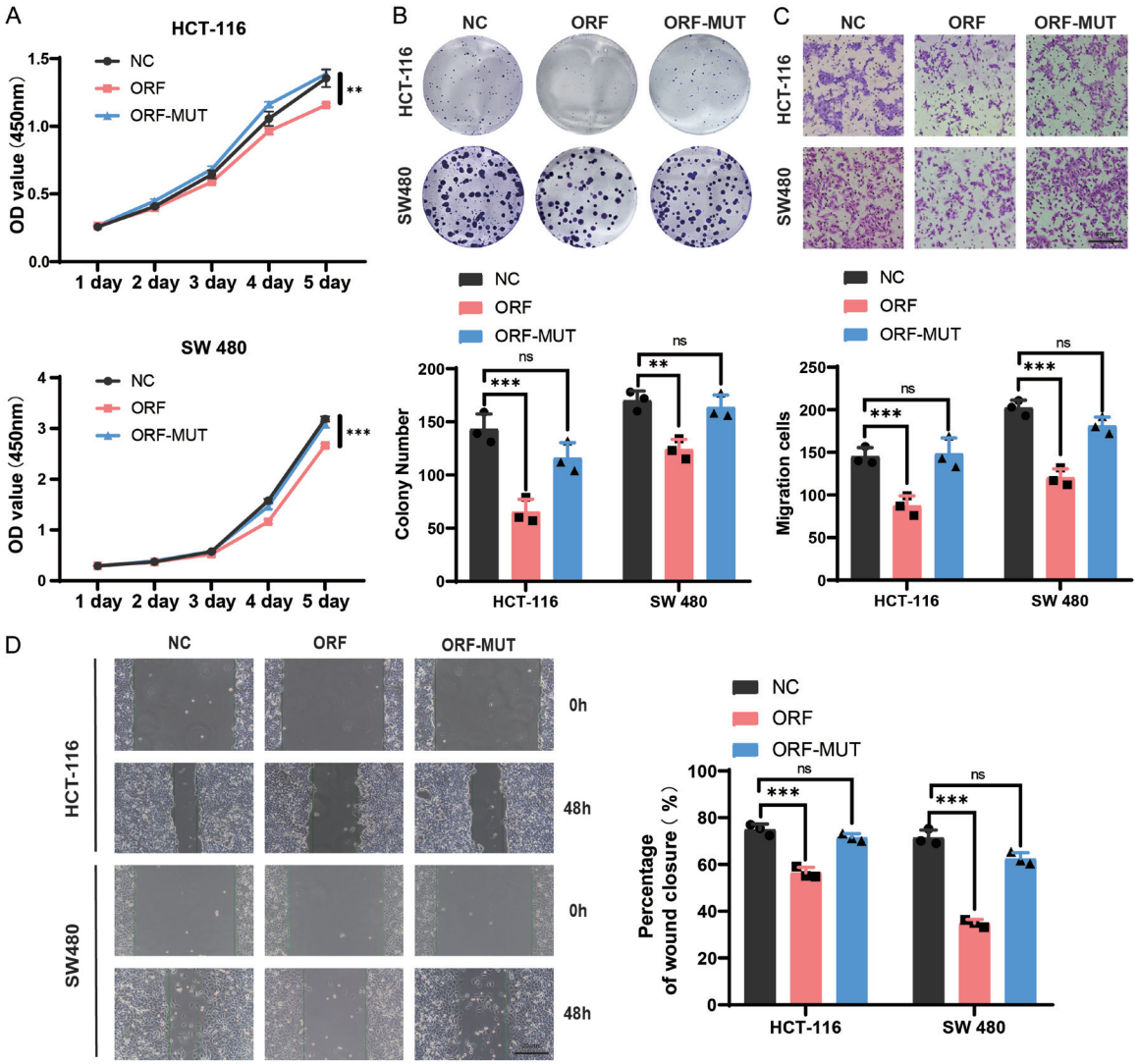

Figure 3. LINC01547-ORF is not an lncRNA but inhibits CRC cells proliferation and migration. Plasmids pcDNA3.1-NC, pcDNA3.1-3xFlag, and pcDNA3.1-3xFlag-mut were transfected into CRC cell lines HCT-116 and SW480 with low expression of LINC01547. Cell proliferation and migration abilities were measured using CCK8, colony formation, transwell migration, and wound healing assays (A-D), with statistical analysis performed. *P < 0.05, **P < 0.01, ***P < 0.001.

HCT-116 and SW480 and the expression of CLDN18 was validated using western blot, RT-qPCR, and IF. The results showed that there was no difference in RNA level between LINC01547-ORF and CLDN18. Due to the stability of transcriptional regulation mechanism and the influence of intracellular negative feedback mechanism, the abundance of CLDN18 mRNA remained unchanged (**Figure 4F**). The expression of CLDN18 protein was up-regulated after overexpression of LINC01547-ORF. LINC01547-ORF inhibits the degradation of CLDN18, causing the protein to accumulate in the cell. The expression of CLDN18 protein was positively correlated with LINC01547-ORF (***P < 0.001, **Figure 4E**, **4G**).

LINC01547-ORF binds to CLDN18 and promotes its protein expression

To identify the interaction domain between LINC01547-ORF and CLDN18 protein, various truncation mutants of CLDN18 were developed (**Figure 5A**). The truncation mutants (1: CLDN18 1-190; 2: CLDN18 191-261) were immunoprecipitated using Flag-tagged pcDNA3.1-3xFlag plasmid and Flag antibody, which showed that

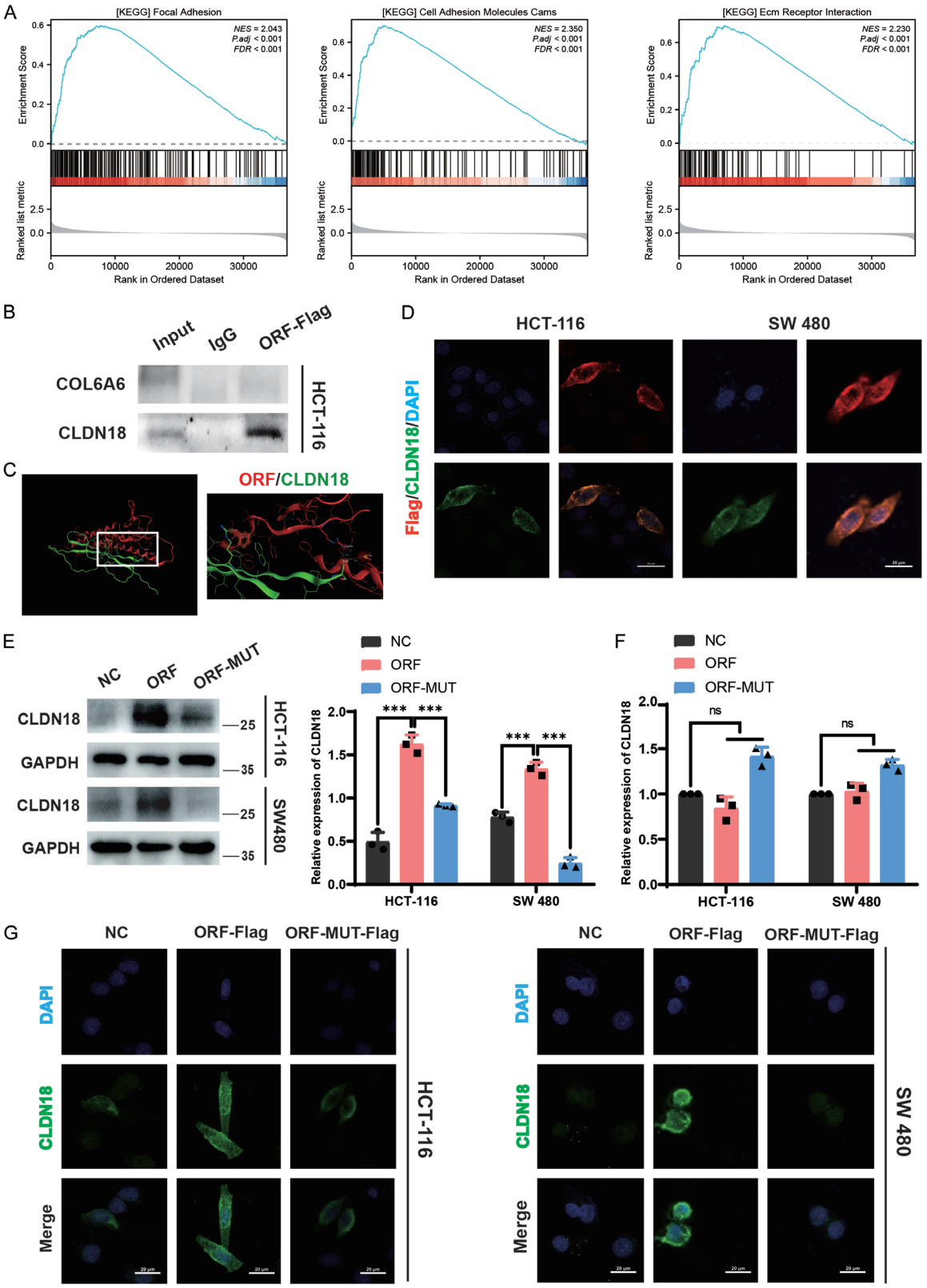

Figure 4. LINC01547-ORF binds to CLDN18 protein. A. Enrichment analysis (GSEA) indicates a relationship between focal adhesion, extracellular matrix, and cell adhesion molecule pathways with LINC01547-ORF. B. Co-IP validated the interaction between LINC01547-ORF and CLDN18 protein, as well as COL6A6 protein. C. Construction of a protein docking model. D. Immunofluorescence experiments confirmed the co-localization of LINC01547-ORF with

CLDN18 protein. E. Western blot analysis verified the correlation between CLDN18 protein and LINC01547-ORF. F. RT-qPCR was used to validate the correlation between CLDN18 and LINC01547-ORF. G. CLDN18 antibody was used to detect the fluorescence expression of LINC01547-ORF in HCT-116 and SW480 cell lines.

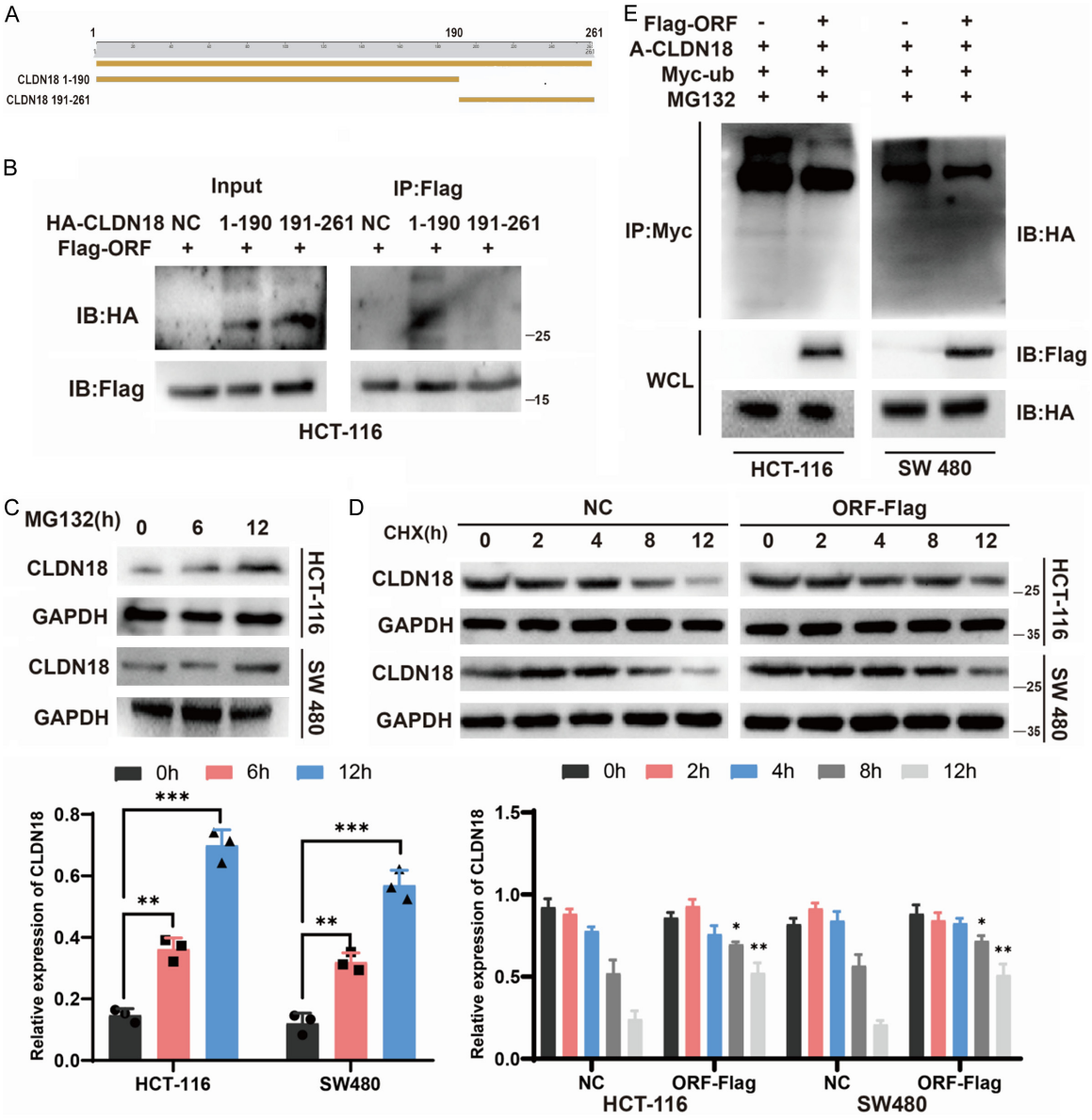

Figure 5. LINC01547-ORF binds to CLDN18 and promotes its protein expression. A. Construction of truncation mutants of different segments of CLDN18 (1: CLDN18 1-190; 2: CLDN18 191-261). B. Co-immunoprecipitation (COIP) analysis of the interaction between LINC01547-ORF and the truncation mutants of CLDN18. C. After treatment with the proteasome inhibitor MG132 for varying hours, the levels of CLDN18 protein regulated by LINC01547-ORF in HCT-116 and SW480 cells were verified. D. Expression of protein in HCT-116 and SW480 cells pre-treated with CHX (50 μg/mL) for different hours was detected by Western blot. E. Co-immunoprecipitation was used to verify the ubiquitination level of CLDN18 regulated by LINC01547-ORF.

the interaction with LINC01547-ORF was mediated by CLDN18 1-190 amino acids (**Figure 5B**). Because LINC01547-ORF promoted CLDN18 protein expression, whether LINC01547-ORF affects CLDN18 ubiquitination was next assessed. After treatment with the proteasome inhibitor MG132, western blot showed that CLDN18 protein level was significantly

increased in HCT-116 and SW480 cells (**P < 0.01, ***P < 0.001, **Figure 5C**). Moreover, in HCT-116 and SW480 cells overexpressing LINC01547-ORF treated with the protein synthesis inhibitor cycloheximide for various times, western blot revealed a significant increase in protein levels compared with the control group (*P < 0.05, **P < 0.01, **Figure 5D**). We added MG132 to prevent its proteasome degradation, and added CLDN18 and LINC01547-ORF to observe the ubiquitination of CLDN18 in HCT-116 and SW480 cells. The results showed that the ubiquitization of CLDN18 decreased significantly after overexpression of LINC01547-ORF. Co-IP experiments confirmed that CLDN18 ubiquitination was mediated by LINC01547-ORF in HCT-116 and SW480 cells (**Figure 5E**).

LINC01547-ORF regulates CLDN18 to inhibit CRC cell proliferation and migration

To evaluate the function of LINC01547-ORF in regulating CLDN18 in CRC, clinical tissue samples were collected and IHC was performed to measure CLDN18 expression in CRC and adjacent healthy tissues. The results showed that CLDN18 expression was downregulated in CRC tissues compared with adjacent healthy tissues (**Figure 6A**). si-NC and si-CLDN18 were transfected into CRC cell lines HCT-116 and SW480, and Western blot analysis showed that the protein expression of CLDN18 was significantly reduced (**P < 0.01, ***P < 0.001, **Figure 6B**). To investigate the effect of CLDN18 on CRC cell lines, the expression of CLDN18 was silenced. Cell function experiments showed that CLDN18 silencing promoted the proliferation and migration of CRC cell lines (**P < 0.01, ***P < 0.001, Figure S1A-D). The results showed that CLDN18 inhibited the proliferation and migration of CRC cell lines. Upon LINC01547-ORF (pcDNA3.1-3xFlag) overexpression and CLDN18 downregulation in CRC cell lines, cell function experiments performed to assess proliferation and migration (*P < 0.05, **P < 0.01, ***P < 0.001, **Figure 6C-F**) indicated that CLDN18 downregulation reversed the inhibitory effect of LINC01547-ORF on HCT-116 and SW480 cells.

LINC01547-ORF inhibits CRC cell growth by regulating CLDN18 and targeting the FAK/PI3K/AKT pathway

Enrichment analysis suggested a relationship of the focal adhesion pathway, ECM, and cell adhesion molecule signaling pathway with LINC01547-ORF (**Figure 4A**). The results showed that LINC01547-ORF binds to the focal adhesion pathway CLDN18 protein (**Figure 4B-D**). Meanwhile, tumor invasion and metastasis are highly correlated with FAK phosphorylation. To identify the target of LINC01547-ORF in inhibiting proliferation and migration after regulating CLDN18, western blot and IF were performed to analyze the role of LINC01547-ORF in targeting the phosphorylation of FAK. Western blot results indicated that LINC01547-ORF inhibited FAK phosphorylation by targeting CLDN18 protein (*P < 0.05, **P < 0.01, ***P < 0.001, **Figure 7A**) and IF revealed a significant decrease in FAK phosphorylation expression due to LINC01547-ORF (**Figure 7B**), suggesting that LINC01547-ORF inhibits FAK phosphorylation via CLDN18 regulation.

In the search for downstream pathways, FAK phosphorylation can activate EMT pathway. Therefore, the epithelial-mesenchymal transition pathway was assessed. The results showed no significant changes in the expression of the mesenchymal markers vimentin and E-cadherin in ORF and ORF+si-CLDN18 groups (*P < 0.05, **P < 0.01, ***P < 0.001, **Figure 7C**). After activation, FAK phosphorylation can activate PI3K, which, in turn, activates AKT and regulates cell growth. Western blot revealed that the expression level of p-PI3K/PI3K and p-AKT/AKT was significantly reduced and that inhibition was particularly strong (*P < 0.05, **P < 0.01, ***P < 0.001, **Figure 7D**). The results show that LINC01547-ORF can inhibit the FAK/PI3K/AKT signaling pathway, and the silencing of CLDN18 reverses the influence of LINC01547-ORF on the FAK/PI3K/AKT signaling pathway. In summary, LINC01547-ORF inhibited CRC cell growth by regulating CLDN18 and targeting the FAK/PI3K/AKT pathway.

Discussion

lncRNAs are a class of eukaryotic RNA molecules that exceed 200 nucleotides in length and do not code for proteins. Recent studies [14, 15, 33-36] have revealed that these lncRNAs may contain one or several short ORFs, potentially encoding microproteins of < 100 amino acids. Because to the small molecular weight of these microproteins and the limitations of conservation analysis-based screening mechanisms and detection techniques,

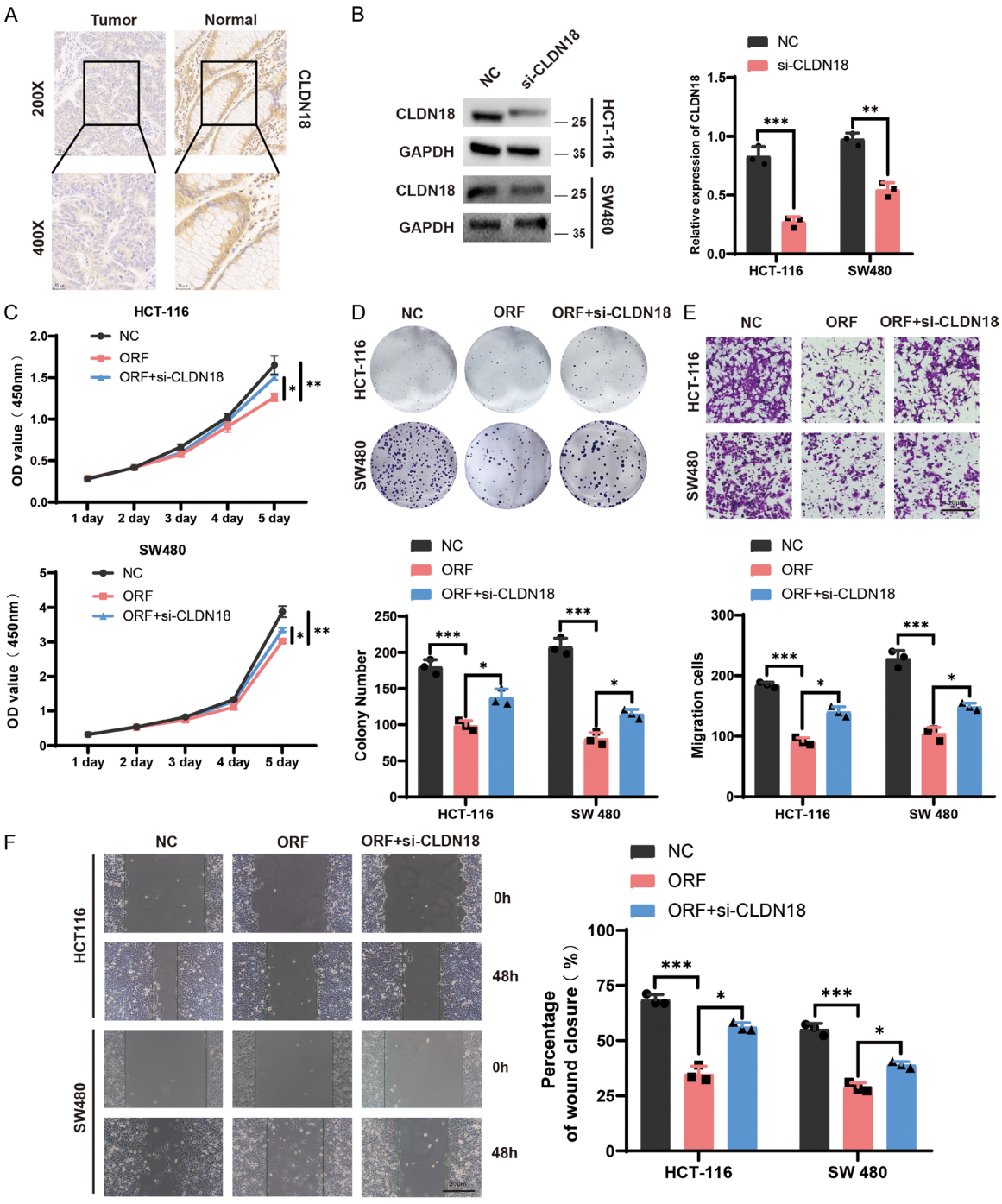

Figure 6. LINC01547-ORF regulates CLDN18 to inhibit CRC cell proliferation and migration. A. Clinical tissue samples were collected and analyzed for the expression of CLDN18 in colorectal cancer tissues and normal adjacent tissues using immunohistochemistry. B. Western blot analysis was used to verify the protein expression of si-CLDN18. C-F. Upon overexpression of LINC01547-ORF, the level of CLDN18 in colorectal cancer cell lines was downregulated, and the effect was verified using CCK8 cell proliferation, colony formation, transwell migration, and wound healing assays. *P < 0.05, **P < 0.01, ***P < 0.001.

these microproteins are often overlooked. This oversight may keep many crucial regulatory mechanisms “hidden”. Thus, the characterization of these microproteins is particularly important [37]. In the present study, LINC01547 was identified to harbor the ability to encode a

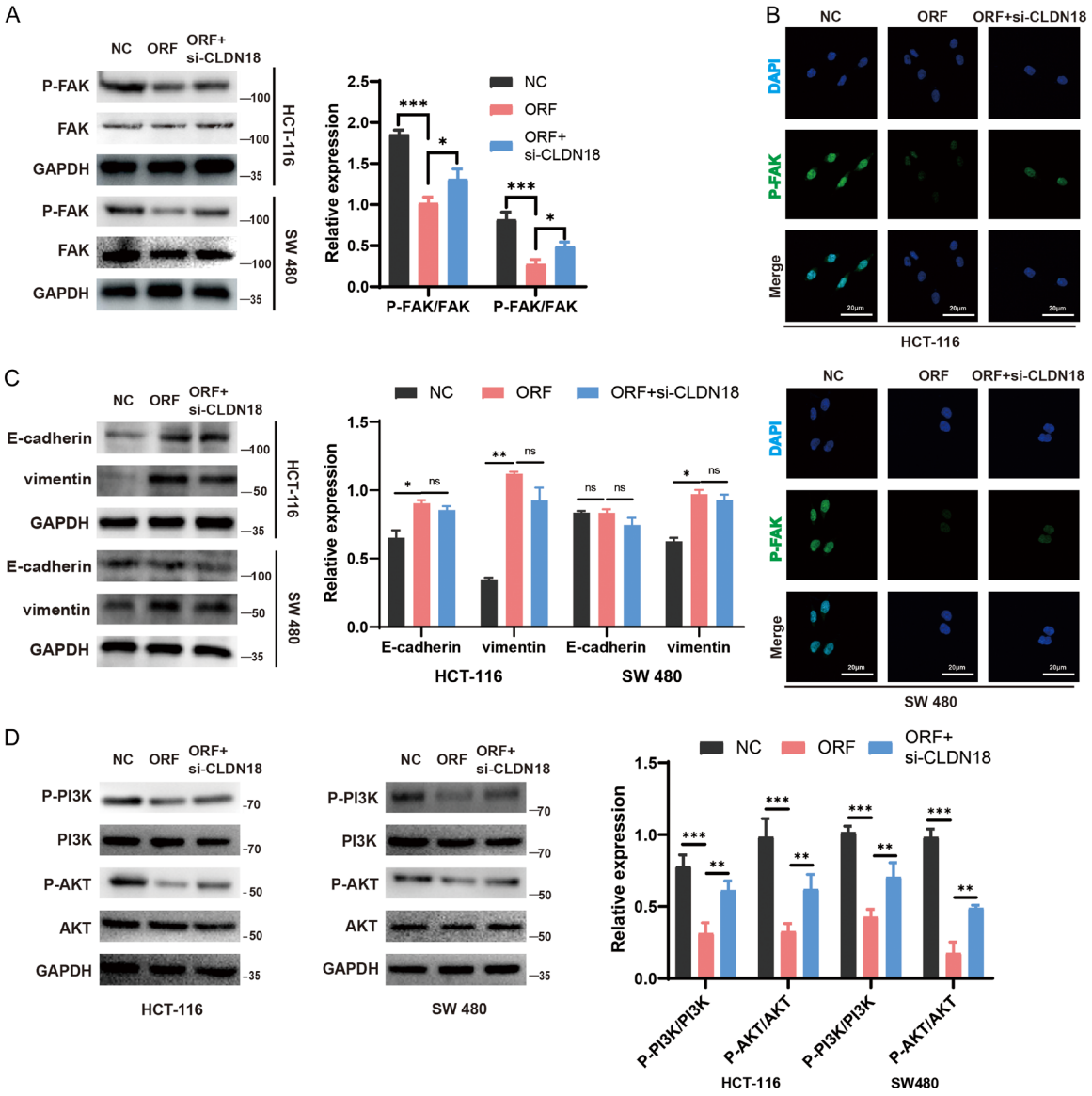

Figure 7. LINC01547-ORF inhibits CRC cell growth by regulating CLDN18 and targeting the FAK/PI3K/AKT pathway. A. Upon overexpression of LINC01547-ORF, the level of CLDN18 in colorectal cancer was downregulated, and the expression of FAK phosphorylation was detected by Western blot. B. Immunofluorescence experiments were further used to detect the correlation between LINC01547-ORF and FAK phosphorylation, using P-FAK antibodies to stain the cells. C. Western blot analysis was performed to detect the expression of the mesenchymal markers vimentin and E-cadherin. D. Western blot analysis was used to test the expression of P-PI3K/PI3K and P-AKT/AKT.

microprotein. Indeed, western blot and IF experiments revealed that LINC01547 could encode the 76-amino-acid microprotein LINC01547-ORF. Cell function assays showed that LINC01547-ORF inhibited the proliferation and migration of the CRC cell lines HCT-116 and SW480.

Existing research has shown that in various tumors, proteins can regulate tumor growth by targeting other proteins [15, 35, 36]. Recent studies have also shown that microproteins encoded by lncRNAs can exert their functions through interactions with others proteins [14, 35, 36, 38]. Therefore, it was hypothesized that LINC01547-ORF inhibits CRC growth through a similar mechanism. To test this hypothesis, GSEA was performed, and the results indicated that the focal adhesion pathway, ECM receptor interaction pathway, and cell adhesion mole-

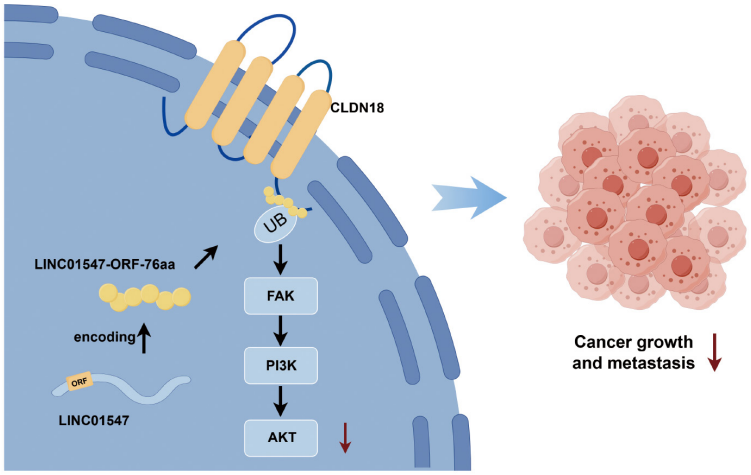

Figure 8. Schematic representation of the data.

cule pathway are closely related to LINC01547-ORF [39]. The protein CLDN18 from the focal adhesion pathway and COL6A6 from the ECM protein collagen VI family were selected for subsequent assessments. Co-IP performed to assess the relationship between LINC01547-ORF and CLDN18/COL6A6 protein suggested that LINC01547-ORF interacts with only the CLDN18 protein. Subsequently, IF experiments revealed that LINC01547-ORF and CLDN18 protein colocalized in the cytoplasm.

Ubiquitination plays a pivotal role in protein covalent modification as well as in maintaining protein homeostasis, participating in protein localization and translocation, and regulating protein activity and related functions, thereby enabling the cell to respond rapidly and sensitively to both external and internal stimuli [40-43]. In particular, protein ubiquitination modifications are extensively involved in several pathophysiological processes, such as the cell cycle, apoptosis, and transcription factor regulation. The regulation of CLDN18 by LINC01547-ORF in CRC was assessed using cell function assays, which showed that CLDN18 downregulation reversed the inhibitory effect of LINC01547-ORF on the CRC cell lines HCT-116 and SW480. These results suggest that LINC01547-ORF regulates CLDN18 to inhibit CRC progression. It is reported that CLDN18-mediated signaling pathways inhibit tumor progression [23, 24]. Therefore, it was hypothesized that LINC01547-ORF inhibits CRC development by suppressing downstream pathways.

During the search for relevant downstream pathways, GSEA identified the focal adhesion pathway, ECM receptor interaction pathway, and cell adhesion molecule pathway. It has been reported that tumor invasion and metastasis are highly correlated with FAK phosphorylation [25, 26]. Western blot and IF experiments confirmed that LINC01547-ORF was closely associated with FAK phosphorylation. To explore additional downstream pathways, epithelial-mesenchymal transition pathway was assessed. However, western blot analysis revealed no significant expression changes in the mesenchymal markers vimentin and E-cadherin. On activation, FAK phosphorylation can activate PI3K and subsequently AKT, thereby regulating cell growth [26]. Therefore, the key genes p-PI3K and p-AKT were evaluated, and the results showed that LINC01547-ORF inhibited the FAK/PI3K/AKT signaling pathway by targeting CLDN18, thereby inhibiting CRC development.

In summary, the study findings suggest that LINC01547 encodes the 76-amino-acid microprotein LINC01547-ORF, which can regulate CLDN18 protein to target and inhibit the FAK/PI3K/AKT pathway, ultimately suppressing CRC cell migration and proliferation (**Figure 8**). To our knowledge, this study confirmed the ability of LINC01547 to encode a microprotein and inhibit CRC cell proliferation and migration. Finally, it was hypothesized that the antitumor effect of LINC01547 on CRC is related to its encoded microprotein, offering a promising direction for the clinical treatment of CRC.

Acknowledgements

This study was supported by the Department of Science and Technology of Henan Province (Grant No. 222102310018), Joint Construction Project of Henan Medical Science and Technology Research Plan (Grant No. LHGJ2021-0910), and the Xinxiang Medical University Research Funding (Grant No. XYBSKYZZ20-1632). We would like to thank for manager Zhu

of the Henan Write gene Biotechnology CO., LTD. for his technical guidance.

All samples were obtained with informed consent from patients with colorectal cancer.

Disclosure of conflict of interest

None.

Abbreviations

CRC, Colorectal cancer; ECM, The extracellular matrix receptor; FAK, Focal adhesion kinase; EMT, epithelial-mesenchymal transition; PI3K, Phosphatidylinositide 3-kinase.

Address correspondence to: Hongwei Chen, Department of Emergency Center Emergency Critical Care, The Fourth Clinical College of Xinxiang Medical College, Xinxiang 453003, Henan, China. Tel: +86-13639890727; E-mail: 1205808181@qq.com; Zheying Zhang, Department of Pathology, School of Basic Medical Sciences, Xinxiang Medical University, Xinxiang 453003, Henan, China. Tel: +86-18903739943; E-mail: 081023@xxmu.edu.cn

References

[1] Xi Y and Xu P. Global colorectal cancer burden in 2020 and projections to 2040. Transl Oncol 2021; 14: 101174.
[2] White MT and Sears CL. The microbial landscape of colorectal cancer. Nat Rev Microbiol 2024; 22: 240-254.
[3] Chan JJ and Tay Y. Noncoding RNA:RNA regulatory networks in cancer. Int J Mol Sci 2018; 19: 1310.
[4] Wu P, Mo Y, Peng M, Tang T, Zhong Y, Deng X, Xiong F, Guo C, Wu X, Li Y, Li X, Li G, Zeng Z and Xiong W. Emerging role of tumor-related functional peptides encoded by lncRNA and circRNA. Mol Cancer 2020; 19: 22.
[5] Chen LL. Linking long noncoding RNA localization and function. Trends Biochem Sci 2016; 41: 761-772.
[6] Ransohoff JD, Wei Y and Khavari PA. The functions and unique features of long intergenic non-coding RNA. Nat Rev Mol Cell Biol 2018; 19: 143-157.
[7] Djebali S, Davis CA, Merkel A, Dobin A, Lassmann T, Mortazavi A, Tanzer A, Lagarde J, Lin W, Schlesinger F, Xue C, Marinov GK, Khatun J, Williams BA, Zaleski C, Rozowsky J, Roder M, Kokocinski F, Abdelhamid RF, Alioto T, Antoshechkin I, Baer MT, Bar NS, Batut P, Bell K, Bell I, Chakrabortty S, Chen X, Chrast J, Curado J, Derrien T, Drenkow J, Dumais E, Dumais J, Duttagupta R, Falconnet E, Fastuca M, Fejes-Toth K, Ferreira P, Foissac S, Fullwood MJ, Gao H, Gonzalez D, Gordon A, Gunawardena H, Howald C, Jha S, Johnson R, Kapranov P, King B, Kingswood C, Luo OJ, Park E, Persaud K, Preall JB, Ribeca P, Risk B, Robyr D, Sammeth M, Schaffer L, See LH, Shahab A, Skancke J, Suzuki AM, Takahashi H, Tilgner H, Trout D, Walters N, Wang H, Wrobel J, Yu Y, Ruan X, Hayashizaki Y, Harrow J, Gerstein M, Hubbard T, Reymond A, Antonarakis SE, Hannon G, Giddings MC, Ruan Y, Wold B, Carninci P, Guigo R and Gingeras TR. Landscape of transcription in human cells. Nature 2012; 489: 101-108.
[8] ENCODE Project Consortium. An integrated encyclopedia of DNA elements in the human genome. Nature 2012; 489: 57-74.
[9] Chen XY, Li MW, Wang Y, Chen Q and Xu HM. Progress on sORF-encoded micropeptides. Yi Chuan 2021; 43: 737-746.
[10] Choi SW, Kim HW and Nam JW. The small peptide world in long noncoding RNAs. Brief Bioinform 2019; 20: 1853-1864.
[11] Li J, Qu L, Sang L, Wu X, Jiang A, Liu J and Lin A. Micropeptides translated from putative long non-coding RNAs. Acta Biochim Biophys Sin (Shanghai) 2022; 54: 292-300.
[12] Makarewich CA and Olson EN. Mining for micropeptides. Trends Cell Biol 2017; 27: 685-696.
[13] Tharakan R and Sawa A. Minireview: novel micropeptide discovery by proteomics and deep sequencing methods. Front Genet 2021; 12: 651485.
[14] Huang JZ, Chen M, Chen D, Gao XC, Zhu S, Huang H, Hu M, Zhu H and Yan GR. A peptide encoded by a putative lncRNA HOXB-AS3 suppresses colon cancer growth. Mol Cell 2017; 68: 171-184, e176.
[15] Guo B, Wu S, Zhu X, Zhang L, Deng J, Li F, Wang Y, Zhang S, Wu R, Lu J and Zhou Y. Micropeptide CIP2A-BP encoded by LINC00665 inhibits triple-negative breast cancer progression. EMBO J 2020; 39: e102190.
[16] Vitorino R, Guedes S, Amado F, Santos M and Akimitsu N. The role of micropeptides in biology. Cell Mol Life Sci 2021; 78: 3285-3298.
[17] Khan MR, Avino M, Wellinger RJ and Laurent B. Distinct regulatory functions and biological roles of lncRNA splice variants. Mol Ther Nucleic Acids 2023; 32: 127-143.
[18] Li M, Wang Y, Li M, Wu X, Setrerrahmane S and Xu H. Integrins as attractive targets for cancer therapeutics. Acta Pharm Sin B 2021; 11: 2726-2737.
[19] Campbell ID and Humphries MJ. Integrin structure, activation, and interactions. Cold Spring Harb Perspect Biol 2011; 3: a004994.

[20] Shah PP, Fong MY and Kakar SS. PTTG induces EMT through integrin alphaVbeta3-focal adhesion kinase signaling in lung cancer cells. Oncogene 2012; 31: 3124-3135.
[21] Chen J, Xu Z, Hu C, Zhang S, Zi M, Yuan L and Cheng X. Targeting CLDN18.2 in cancers of the gastrointestinal tract: new drugs and new indications. Front Oncol 2023; 13: 1132319.
[22] Cao W, Xing H, Li Y, Tian W, Song Y, Jiang Z and Yu J. Claudin18.2 is a novel molecular biomarker for tumor-targeted immunotherapy. Biomark Res 2022; 10: 38.
[23] Luo J, Chimge NO, Zhou B, Flodby P, Castaldi A, Firth AL, Liu Y, Wang H, Yang C, Marconett CN, Crandall ED, Offringa IA, Frenkel B and Borok Z. CLDN18.1 attenuates malignancy and related signaling pathways of lung adenocarcinoma in vivo and in vitro. Int J Cancer 2018; 143: 3169-3180.
[24] Xu X, Li Y, Zhang R, Chen X, Shen J, Yuan M, Chen Y, Chen M, Liu S, Wu J and Sun Q. Jianpi Yangzheng decoction suppresses gastric cancer progression via modulating the miR-448/CLDN18.2 mediated YAP/TAZ signaling. J Ethnopharmacol 2023; 311: 116450.
[25] Li S and Hua ZC. FAK expression regulation and therapeutic potential. Adv Cancer Res 2008; 101: 45-61.
[26] Narayanankutty A. PI3K/Akt/mTOR pathway as a therapeutic target for colorectal cancer: a review of preclinical and clinical evidence. Curr Drug Targets 2019; 20: 1217-1226.
[27] Gan B, Yoo Y and Guan JL. Association of focal adhesion kinase with tuberous sclerosis complex 2 in the regulation of s6 kinase activation and cell growth. J Biol Chem 2006; 281: 37321-37329.
[28] Zheng D, Duan H, Wang S, Xu Q, Gan L, Li J and Dong Q. FAK regulates epithelial-mesenchymal transition in adenomyosis. Mol Med Rep 2018; 18: 5461-5472.
[29] Luo J, Yao JF, Deng XF, Zheng XD, Jia M, Wang YQ, Huang Y and Zhu JH. 14, 15-EET induces breast cancer cell EMT and cisplatin resistance by up-regulating integrin alphavbeta3 and activating FAK/PI3K/AKT signaling. J Exp Clin Cancer Res 2018; 37: 23.
[30] Zhang C, Yu Z, Yang S, Liu Y, Song J, Mao J, Li M and Zhao Y. ZNF460-mediated circRPPH1 promotes TNBC progression through ITGA5-induced FAK/PI3K/AKT activation in a ceRNA manner. Mol Cancer 2024; 23: 33.
[31] Zhu W, Wu C, Liu Z, Zhao S, Cheng X and Huang J. SULF1 regulates malignant progression of colorectal cancer by modulating ARSH via FAK/PI3K/AKT/mTOR signaling. Cancer Cell Int 2024; 24: 201.
[32] Livak KJ and Schmittgen TD. Analysis of relative gene expression data using real-time quantitative PCR and the 2-ΔΔCT method. Methods 2001; 25: 402-408.
[33] Ge Q, Jia D, Cen D, Qi Y, Shi C, Li J, Sang L, Yang LJ, He J, Lin A, Chen S and Wang L. Micropeptide ASAP encoded by LINC00467 promotes colorectal cancer progression by directly modulating ATP synthase activity. J Clin Invest 2021; 131: e152911.
[34] Wu S, Guo B, Zhang L, Zhu X, Zhao P, Deng J, Zheng J, Li F, Wang Y, Zhang S, Zhang Z, Lu J and Zhou Y. A micropeptide XBP1SBM encoded by lncRNA promotes angiogenesis and metastasis of TNBC via XBP1s pathway. Oncogene 2022; 41: 2163-2172.
[35] Zhang C, Zhou B, Gu F, Liu H, Wu H, Yao F, Zheng H, Fu H, Chong W, Cai S, Huang M, Ma X, Guo Z, Li T, Deng W, Zheng M, Ji Q, Zhao Y, Ma Y, Wang QE, Tang TS and Guo C. Micropeptide PACMP inhibition elicits synthetic lethal effects by decreasing CtIP and poly(ADP-ribosyl)ation. Mol Cell 2022; 82: 1297-1312, e1298.
[36] Yang JE, Zhong WJ, Li JF, Lin YY, Liu FT, Tian H, Chen YJ, Luo XY and Zhuang SM. LINC00998-encoded micropeptide SMIM30 promotes the G1/S transition of cell cycle by regulating cytosolic calcium level. Mol Oncol 2023; 17: 901-916.
[37] Ruiz-Orera J and Alba MM. Translation of small open reading frames: roles in regulation and evolutionary innovation. Trends Genet 2019; 35: 186-198.
[38] Li M, Liu G, Jin X, Guo H, Setrerrahmane S, Xu X, Li T, Lin Y and Xu H. Micropeptide MIAC inhibits the tumor progression by interacting with AQP2 and inhibiting EREG/EGFR signaling in renal cell carcinoma. Mol Cancer 2022; 21: 181.
[39] Canzler S and Hackermuller J. multiGSEA: a GSEA-based pathway enrichment analysis for multi-omics data. BMC Bioinformatics 2020; 21: 561.
[40] Popovic D, Vucic D and Dikic I. Ubiquitination in disease pathogenesis and treatment. Nat Med 2014; 20: 1242-1253.
[41] Swatek KN, Usher JL, Kueck AF, Gladkova C, Mevissen TET, Pruneda JN, Skern T and Komander D. Insights into ubiquitin chain architecture using Ub-clipping. Nature 2019; 572: 533-537.
[42] Martinez-Ferriz A, Ferrando A, Fathinajafabadi A and Farras R. Ubiquitin-mediated mechanisms of translational control. Semin Cell Dev Biol 2022; 132: 146-154.
[43] Liu J, Zhang C, Xu D, Zhang T, Chang CY, Wang J, Liu J, Zhang L, Haffty BG, Zong WX, Hu W and Feng Z. The ubiquitin ligase TRIM21 regulates mutant p53 accumulation and gain of function in cancer. J Clin Invest 2023; 133: e164354.

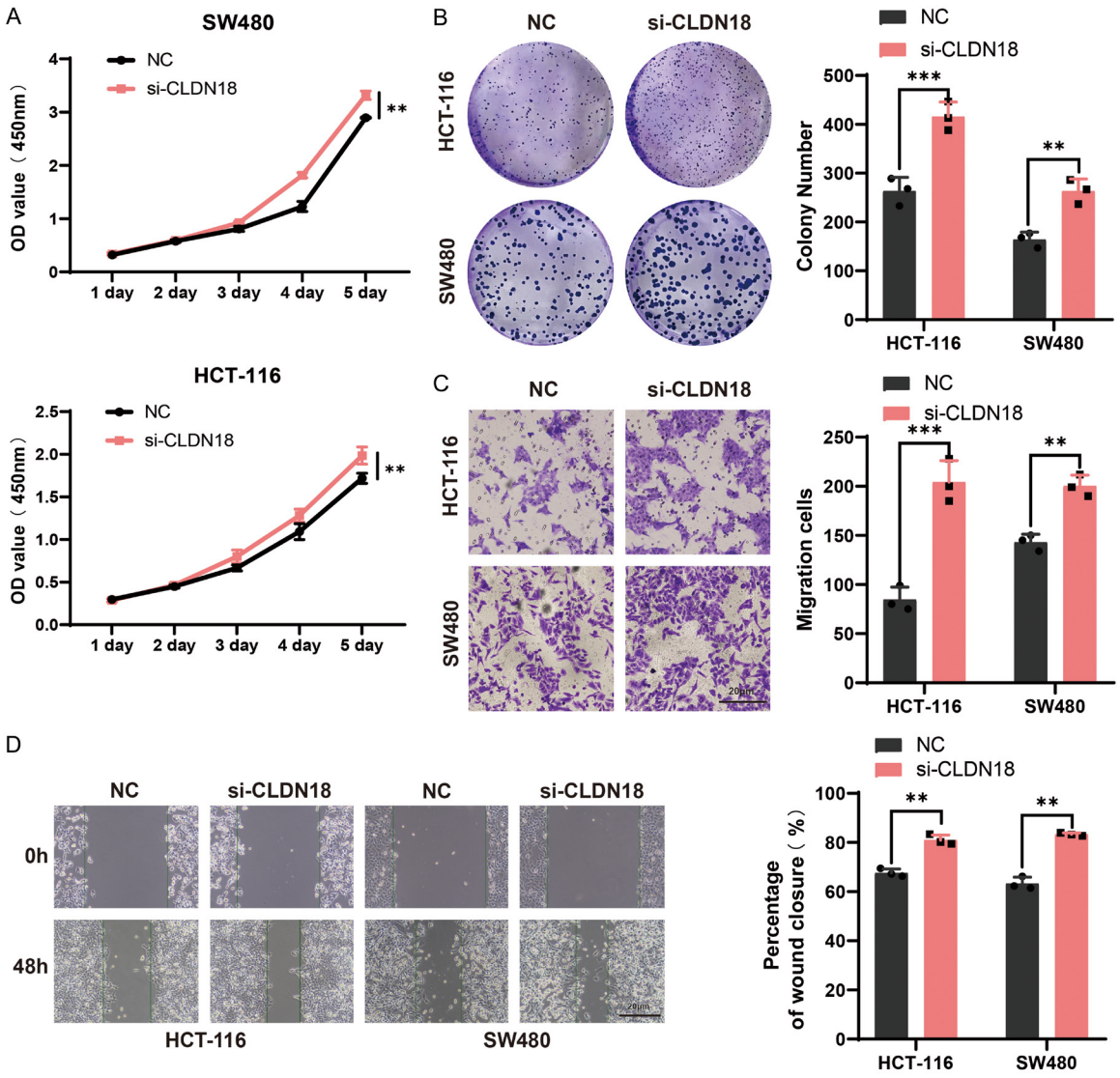

Figure S1. CLDN18 inhibits CRC cell proliferation and migration. si-NC and si-CLDN18 were transfected into colorectal cancer cell lines HCT-116 and SW480, Cell proliferation and migration abilities were measured using CCK8, colony formation, transwell migration, and wound healing assays (A-D), with statistical analysis performed. *P < 0.05, **P < 0.01, ***P < 0.001.